

Decomposition of β -O-4 Linked Lignin Model Compound in Anhydrous Ethanol without any Added Catalyst

Xuezhong Wu,^{a,b} Wenqian Jiao,^a Yanming Li,^b Bing-Zheng Li,^b Yanghuan Huang,^a Hongbin Zhang,^a Yahong Zhang,^a Quanrui Wang,^c and Yi Tang^{a,*}

The cleavage of a lignin model compound of 2-phenoxyacetophenone (2-PAP) was studied in an anhydrous ethanol solvent. A high conversion of 2-PAP (> 99%) to the desired products (> 80% for phenol) with impressive selectivity was achieved in a stainless steel (T316SS) autoclave without any added catalyst. The stainless steel was analyzed as being effective at catalyzing the decomposition of 2-PAP because of its hydrogen transfer activity and stabilization of reaction intermediates, while anhydrous ethanol served as both a solvent and hydrogen donor. An active hydrogen-promoted reaction network was proposed to explain these results. Further investigation demonstrated that the co-catalyst, Cs_{2.5}H_{0.5}PMo₁₂O₄₀, enhanced the cleavage efficiency, which resulted in high yields of the desired products (> 98% of phenol and > 91% of acetophenone). The proposed method in this study based on the stainless steel-promoted hydrogen transfer reaction, which had the merits of a high conversion efficiency and easy handling, can be expected to develop a promising process for further transformation of lignin to valuable multi-substituted aromatics.

Keywords: Stainless steel autoclave; Hydrogen transfer; Lignin model compound; Anhydrous ethanol

Contact information: a: Department of Chemistry, Laboratory of Advanced Materials, Collaborative Innovation Center of Chemistry for Energy Materials and Shanghai Key Laboratory of Molecular Catalysis and Innovative Materials, Fudan University, Shanghai, 200433, China; b: State Key Laboratory of Non-Food Biomass Enzyme Technology, National Engineering Research Center for Non-Food Biorefinery, Guangxi Key Laboratory of Biorefinery, Guangxi Academy of Sciences, Nanning, 530007, China; c: Department of Chemistry, Fudan University, Shanghai, 200433, China;

* Corresponding author: yitang@fudan.edu.cn

INTRODUCTION

With the depletion of fossil fuels and the exacerbation of the greenhouse effect, sustainable development is highlighted by many governments. Some fuels and chemicals produced from renewable resources such as biomass can be plausible and prospected in the future (Bull 1999; Werpy *et al.* 2004; Argyropoulos 2007; van Haveren *et al.* 2008). Lignocellulose biomass is an almost inexhaustible, carbon-neutral, and consistently renewable source of energy and chemicals. As the second principal component of lignocellulose, lignin can be applied as the precursor for many aromatics. However, it is still far from being effectively utilized. At present, most lignin is burned directly as fuel, and only a small portion is used to produce dispersants or adhesives. An even smaller amount is used to produce valuable chemicals (Zakzeski *et al.* 2012; Kang *et al.* 2013; Deuss and Barta 2016). With the increased investigation into lignin structure and development of catalytic technologies, the preparation of bulk or fine aromatics from lignin

is feasible and has attracted considerable interest (Zakzeski *et al.* 2012; Song *et al.* 2013; Deuss and Barta 2016).

Because of its stable spatial network structure and complicated chemical conjunctions of primary monomers, it is a challenge to convert lignin into valuable products (Dutta *et al.* 2014). Some researchers intend to elucidate the mechanism of the decomposition of lignin through the study of cleavage of the model compounds (Yan *et al.* 2010; Song *et al.* 2013; Luo *et al.* 2016). In natural lignin the β -O-4 linkage accounts for approximately 60% of all linkages of primary monomers. 2-Phenoxy-1-phenylethan-1-ol (POPE, Fig. S1 in Supporting Information (SI)) is generally used as a mimic of β -O-4 linkages in lignin because of its abundance in natural lignin (Heitner *et al.* 2010; Deuss and Barta 2016). Some researchers have also selected 2-phenoxy-1-phenylethan-1-one (2-phenoxyacetophenone, 2-PAP, Fig. S1) as a model compound because this linkage represents partially oxidized lignin (Strassberger *et al.* 2013; Zhang *et al.* 2013; Deuss and Barta 2016).

Stainless steel autoclaves are popular in chemistry labs and are often operated at high temperatures and/or under high pressures. Numerous studies of lignin decomposition in stainless steel autoclaves have been recorded (Park *et al.* 2011; Vollhardt and Schore 2011; Zeng *et al.* 2015), and the effects of stainless steel autoclaves on the reactions have also been observed (De Oliveira-Vigier *et al.* 2005; Szpyrkowicz *et al.* 2005), but not much attention has been paid to these phenomena. During some initial experiments with decomposition of 2-PAP in anhydrous ethanol (AE) in a stainless steel autoclave, it was found that the substrate was totally converted without the addition of any catalyst. This meant that the stainless steel of the autoclave wall potentially catalyzed the reaction. Therefore, in this study, 2-PAP was employed as the model compound to explore the catalytic effects of the stainless steel from an autoclave wall.

EXPERIMENTAL

Materials

The model compounds 2-PAP and POPE were purchased from TCI Chemicals (Shanghai, China) and Bide Pharmatech Ltd. (Shanghai, China) and were used as received. Isopropanol (IPA), AE, acetone, benzene, phenol, acetophenone, $\text{H}_3\text{PMo}_{12}\text{O}_{40}\cdot x\text{H}_2\text{O}$, and cesium nitrate (CsNO_3) were all of analytical purity and were offered by Sinopharm Chemical Reagent Co. Ltd. (Shanghai, China). They were used as received without further purification. The stainless steel powder of type 316 (SSP316, particle size ~ 0.08 mm) was kindly provided by Shijiazhuang Jingyuan Power Materials Co. Ltd. (Shijiazhuang, China) and used as a catalyst directly without any treatment.

Preparation of $\text{Cs}_{2.5}\text{H}_{0.5}\text{PMo}_{12}\text{O}_{40}$

The catalyst, $\text{Cs}_{2.5}\text{H}_{0.5}\text{PMo}_{12}\text{O}_{40}$, was prepared by an ion exchange method from $\text{H}_3\text{PMo}_{12}\text{O}_{40}\cdot x\text{H}_2\text{O}$ according to the procedures described by Park *et al.* (2011). The precise quantification of water content in $\text{H}_3\text{PMo}_{12}\text{O}_{40}\cdot x\text{H}_2\text{O}$ was analyzed by thermal treatment at 300 °C for 4 h, and the water content was determined to be $\text{H}_3\text{PMo}_{12}\text{O}_{40}\cdot 27\text{H}_2\text{O}$. The solid heteropolyacid catalyst $\text{Cs}_{2.5}\text{H}_{0.5}\text{PMo}_{12}\text{O}_{40}$ was prepared using an ion exchange method. A stoichiometric amount of CsNO_3 was dissolved in deionized water, and then, while vigorously stirring, the solution was added dropwise into an aqueous solution containing $\text{H}_3\text{PMo}_{12}\text{O}_{40}$. The resulting solution was heated slowly (1 °C/min) to 60 °C and

kept at this temperature for 24 h, and a faint yellow solid was obtained. The solid product was dried overnight at 70 °C, and it was then calcined at 250 °C for 4 h in air to yield $C_{S2.5}H_{0.5}PMo_{12}O_{40}$. Finally, the product was kept in a desiccator until it was used.

Decomposition of Lignin Model Compounds

Most of the decomposition reactions were conducted in a T316 stainless steel autoclave (denominated as T316SS with its composition shown in Table S1 in SI) equipped with a controller, a thermocouple, and a mechanical agitator (Model 4598, Parr Instrument Company, Moline, USA). For comparison, some specified reactions were executed in a poly(*p*-phenylene) (PPE)-lined reactor in static or dynamic mode heated in an electric oven. The reactions were typically operated by first dosing 0.100 g of 2-PAP and 0.010 g of catalyst (or none) into the dry autoclave, after which 50 mL of solvent was introduced. The autoclave was closed quickly to prevent adsorbing water, and then purged with N_2 several times. The reaction was performed at 260 °C for 4 h with a stirring speed of 300 rpm. After a predetermined time, the reactor was cooled down to room temperature and the products were collected for further analysis.

Products Analysis

The products were first evaluated by gas chromatograph-mass spectroscopy (GC-MS, Model DSQ II, Thermo Fisher, Austin, USA), and then analyzed using a GC-FID equipped with HP-5 column (GC-2010, Shimadzu, Kyoto, Japan). The concentration of 2-PAP, POPE, phenol, and acetophenone were quantified by the external standard method. The conversion of substrate, the selectivities of phenol and acetophenone, and the total mass yield of all other products (wt.%) were calculated by the following equations,

$$Conv. / \% = \frac{c_{substrate\ before} - c_{substrate\ post}}{c_{substrate\ before}} \times 100 \quad (1)$$

$$S_p / \% = \frac{c_{phenol}}{c_{substrate\ before} \times Conv.} \times 100 \quad (2)$$

$$S_A / \% = \frac{c_{acetophenone}}{c_{substrate\ before} \times Conv.} \times 100 \quad (3)$$

$$Y_{others} / \% = \frac{\omega_{substrate\ before} - \omega_{substrate\ post} - \omega_{phenol} - \omega_{acetophenone}}{\omega_{substrate\ before}} \times 100 \quad (4)$$

where *Conv.* is the conversion of the substrate 2-PAP, S_p and S_A are the selectivities of phenol and acetophenone, respectively, Y_{others} is the total mass yield of the other products than phenol and acetophenone, c is the molar concentration of the specific compound calculated by the chromatographic peak area in the GC-FID chart of reaction products that corresponded to the external standards of a specific compound (mol/L), and ω is the mass concentration of a specified compound (g/L).

Determination of Metals Dissolved in the Solvent

Metals that probably had been leached from the autoclave wall into the solvent were analyzed by Inductively Coupled Plasma-Atomic Emission Spectrometry (ICP-AES, Model iCAP6300, Thermo Fisher, Waltham, USA). About 20 mL of solvent before or after the reaction was withdrawn in a cleaned crucible which was then first acidified by HNO₃ solvent, and then air-dried at room temperature. Then the crucible was calcined at 500 °C for 6 h in air. After that, 20 mL of HNO₃ solvent (1 mol/L) was introduced into the crucible and then the crucible was kept in an ultrasonic machine for 30 min. Finally, the metals in this ultrasonic treated solvent were determined by ICP-AES.

RESULTS AND DISCUSSION

Proofs for 2-PAP Decomposition Promoted by T316SS Reactor

Figures 1A through 1D are the chromatograms of 2-PAP decomposition products in ethanol after it was reacted at 260 °C for 4 h under control conditions. Some semi-quantitative data are also offered in Table 1 as supplement. All the compounds in the products were determined by GC-MS with some of the main products further analyzed by retention time in a GC-FID (Table S2 in SI).

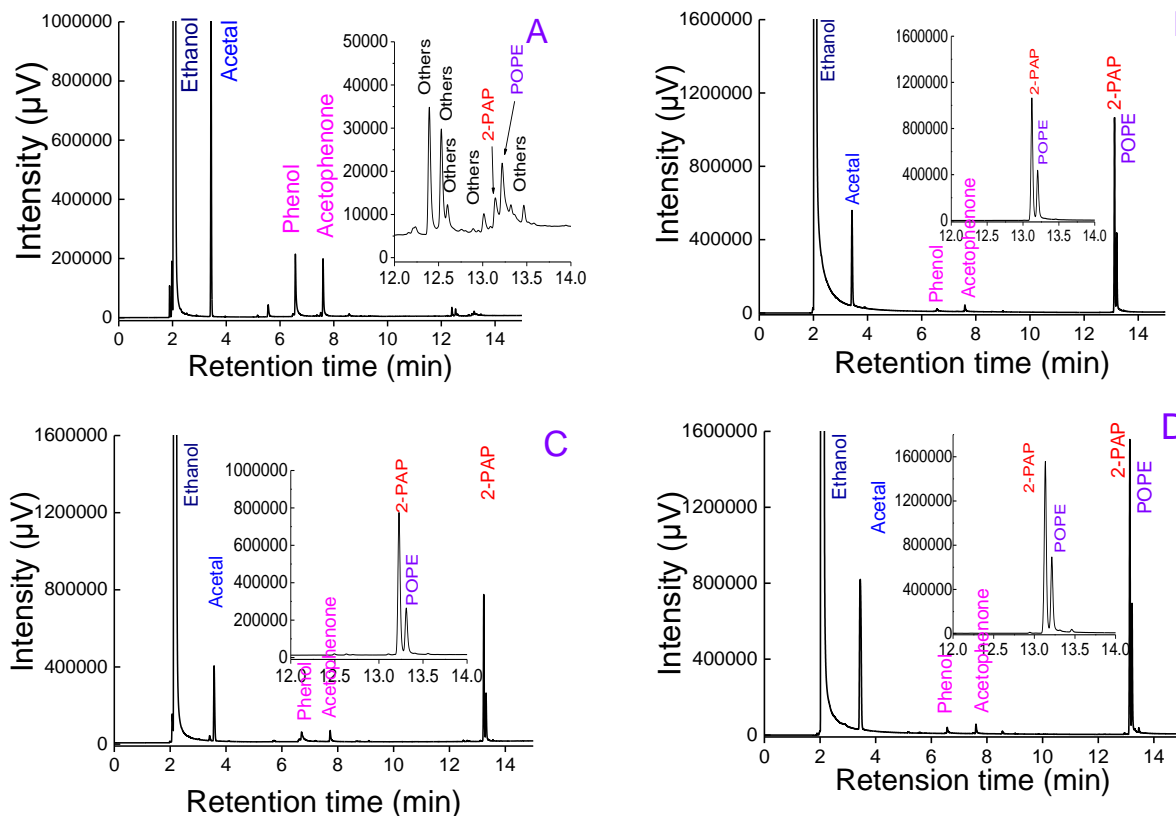


Fig. 1. GC Chromatograms of post-reaction products of 2-PAP in a T316SS autoclave with a stirring speed of 300 rpm (A), 100 rpm (B), 0 rpm (C), and in PPE-lined autoclave at dynamic mode (D). The insets in Fig. 1A-1D are the enlargements of a part of the corresponding chromatogram. Experimental Conditions: substrate: 2-PAP; solvent: anhydrous ethanol; temperature: 260 °C; retention time: 4 h; Catalyst: None.

Table 1. Decomposition Results of Control Reactions of 2-PAP under Various Experimental Conditions*

Figure No.	Experimental Conditions			Products Distribution			
	Autoclave	Mixing Mode	Catalyst	Conv. (%)	A _P (%)	A _A (%)	A _{POPE} (%)
1A	T316SS	Stirring at 300 rpm	None	> 99	40.2	46.0	8.2
1B	T316SS	Stirring at 100 rpm	None	40.2	2.5	3.3	34.4
1C	T316SS	Stirring at 0 rpm	None	45.2	4.1	5.4	25.7
1D	PPE	dynamic mode	None	32.5	2.6	2.9	27.0
S2C	PPE	dynamic mode	SSP316	88.5	5.8	3.1	73.9
S2D	PPE	static mode	SSP316	36.7	5.7	3.4	22.3

*Peak area of chromatograms normalization method. Experimental conditions: substrate: 2-PAP; solvent: AE; temperature: 260 °C; retention time: 4 h.

2-PAP was treated in an AE solvent in a T316SS autoclave without the addition of any catalyst at 260 °C for 4 h with a stirring speed of 300 rpm. The trace of decomposition products is shown in Fig. 1A. Compared with the chromatogram of raw material of 2-PAP displayed in Fig. S2B in SI, the signal at the retention time 13.134 min almost disappeared. Instead, two new peaks appeared at retention times 6.433 and 7.475 min, which were attributed to phenol and acetophenone, respectively. This demonstrated that the transformation of 2-PAP took place with a high selectivity of the desired products (Fig. 1A, Table 1) without the addition of any catalysts.

The possibility of the presence of other catalysts or some other unknown factor impacting the reactions was taken into consideration, and the experiment was repeated several times. The results were easily reproduced (Fig. S3 in SI). It should be noted that the autoclave had not been used by other investigators and no other catalysts were involved during the research period.

Typically, the homolysis of β -O-4 bond (pyrolysis) in the absence of a catalyst occurs only at high temperatures (> 500 °C) because of the high bond dissociation energy of C-O in an ether bond. Therefore, it was inferred that the decomposition of 2-PAP in this study at a relatively low temperature (260 °C) was achieved with a catalyst and that the wall of the T316SS autoclave acted as that catalyst in the cleavage of β -O-4 conjunction.

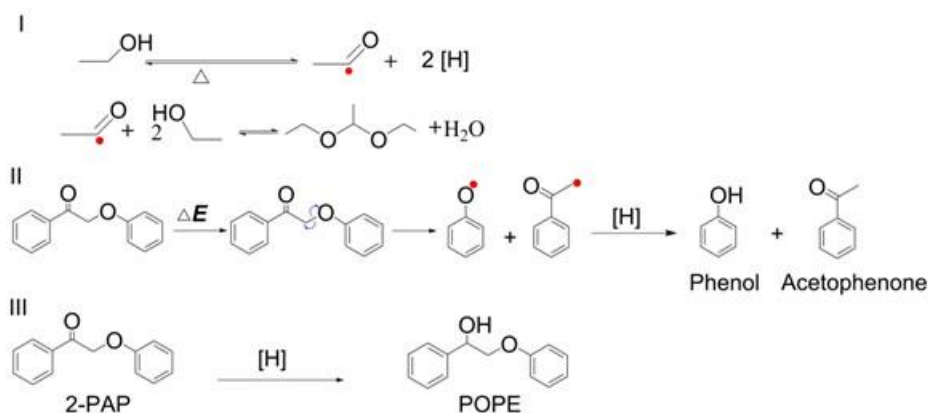
To determine the probability that some metals had been leached from the autoclave wall into the solvent and served as the homogeneous catalyst in this reaction, the amount of metals dissolved in ethanol before and after the reaction was determined by ICP-AES (Table S3 in SI). The results showed that only trace metals were detected in the solvent, and concentrations were almost unchanged before and after the reactions, which meant that only small amounts of metals were leached from the steel wall. Furthermore, when the stirring speed during the reaction was varied, the conversion and selectivity (Fig. 1A-1C) were greatly changed, which happened scarcely in homogeneous reactions. Thus, it was suggested that the catalysis should be ascribed to the steel wall.

To further clarify the catalysis function of the stainless steel wall in these reactions, some comparative experiments were performed in a PPE-lined autoclave in dynamic mode (in a rotary ramp of 100 rpm in electric oven) with and without stainless steel powders (SSP316) as a catalyst, and the experiment results are displayed in Fig. 1D and Fig. S2C in SI, respectively. Comparing Fig. S2C in SI to Fig. 1D (also in Table 1), the addition of SSP316 in the mixture improved the transformation of 2-PAP.

The same reaction was also executed in static mode with SSP316 as a catalyst in a PPE-lined autoclave, and the chromatogram of the obtained products is shown in Fig. S2D in SI. It indicated that stirring further promoted the conversion of 2-PAP, which may have been due to the enhancement of mass/heat transfer effects in dynamic mode (Table 1). To verify this conclusion, experiments were also carried out in a T316SS autoclave at a 100 rpm stirring speed (Fig. 1B) and in static mode (Fig. 1C). It can be clearly seen that lower conversions of 2-PAP were achieved when the reaction was performed in static mode or at a slower stirring speed (Table 1), which indicated that the mass/heat transfer factors were important for the conversion and cleavage of this β -O-4 model compound. It seems that when the stirring speed is over a specialized value (such as 100 rpm in our reaction), the products' distribution can change obviously, as the change of fluent flow state with the variance of Reynolds' Constant.

Moreover, after further analyzing the detailed structures of the products, it was determined that the hydrogen species must have been involved in the conversion of 2-PAP without adding additional hydrogen gas. The main products, phenol and acetophenone, and the by-product, POPE, all have two more hydrogen atoms compared to the raw material of 2-PAP (Line II and III in Scheme 1). Solvents with hydrogen donating capability, such as methanol, ethanol, and formic acid, were employed in the decomposition of the lignin compound (Xu *et al.* 2012; Song *et al.* 2013; Huang *et al.* 2015).

To explore the origin of the hydrogen, pure AE solvent was treated at 260 °C for 4 h in a T316SS autoclave or a PPE-lined autoclave, and their chromatograms are exhibited in Fig. S2E and S2F in SI. Compared with the chromatogram of untreated AE displayed in Fig. S2A in SI, a new peak at retention time 3.437 min (Table S2) appeared in both of the chromatograms (Fig. S2E and S2F in SI). This was ascribed to diethyl acetal (denominated as acetal), which was confirmed by GC-MS. It was easy to infer that during the generation of acetal, ethylal was also produced simultaneously. After further quantification by GC-FID peak area (Fig. S4 in SI), the concentration of ethylal in the pure AE increased remarkably from approximately 0.001% before the reaction to 0.336% after the reaction. Active hydrogen species were released accompanying the generation of acetal and ethylal without the addition of any catalyst (Scheme 1), regardless of whether the reaction occurred in a T316SS autoclave with stirring or in a PPE-lined autoclave in static mode. Thus, AE was the origin of the active hydrogen.



Scheme 1. Pathways of (I) hydrogen generation, (II) decomposition of 2-PAP and hydrogenation, or (III) excessive hydrogenation of model compound 2-PAP

Effects of Solvents

To clarify the effects of solvents with various hydrogen donation capabilities on the transformation of 2-PAP, some exploratory experiments were also performed in various solvents in a T316SS autoclave without the addition of any catalyst at 260 °C for 4 h with a stirring speed of 300 rpm. The total ion current (TIC) GC-MS chromatograms for the products are presented in Fig. S5 in SI, while the corresponding GC-FID chromatograms are presented in Fig. 2.

Table 2. Products Analysis for Decomposition of 2-PAP in Various Solvents*

Entry	Solvent	Conv. (%)	Products Distribution			
			S _P (%)	S _A (%)	S _P /S _A	Others mass yield (wt.%)
1	AE	>99	65.6	40.6	1.6	47.9
2	IPA	>99	84.4	35.4	2.4	42.6
3	Acetone	5.8	0.8	0.7	1.1	5.8
4	Benzene	5.2	0.7	0.8	0.8	5.1

*Experimental conditions: substrate: 2-PAP; reactor: T316SS autoclave with stirring speed of 300 rpm; temperature: 260 °C; time: 4 h; Catalyst: None. Quantified by GC-FID using external standard methods.

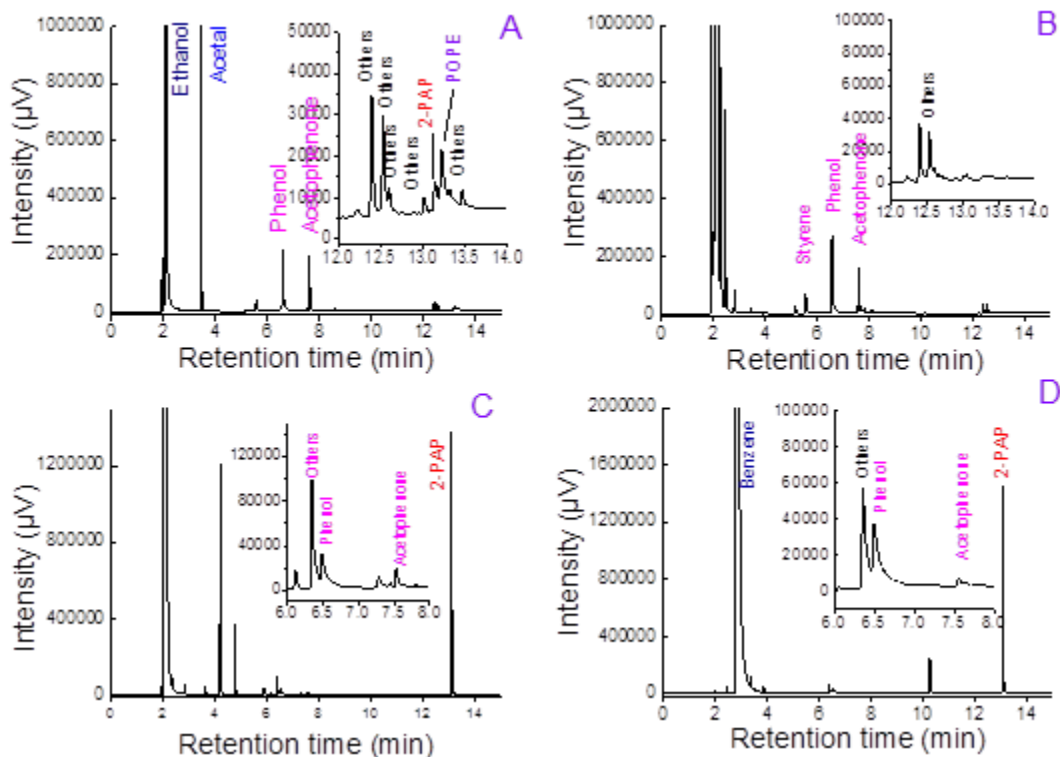
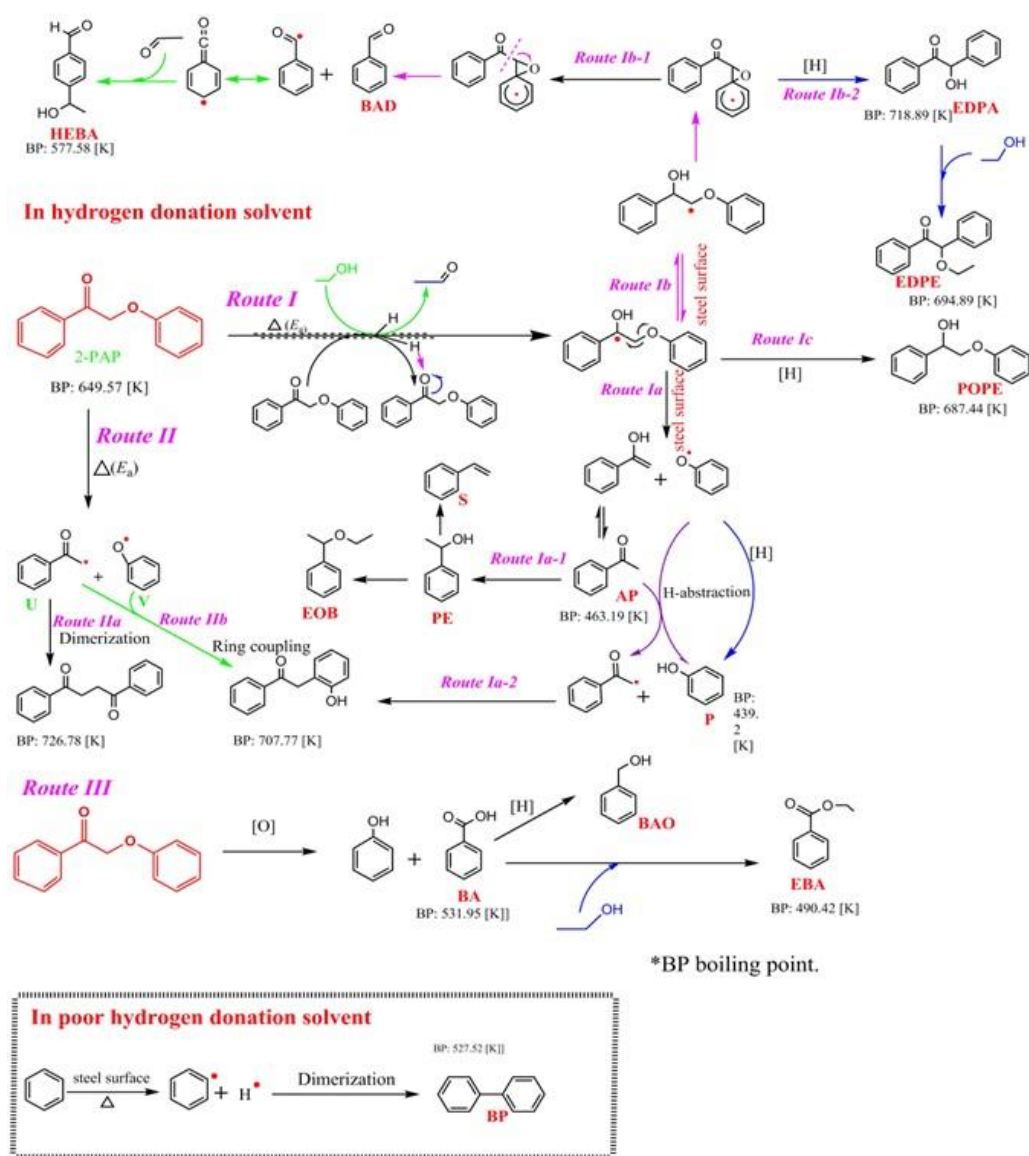


Fig. 2. GC-FID Chromatograms of post-reaction products of 2-PAP in various solvents, where (A) is AE, (B) is IPA, (C) is Acetone, and (D) is Benzene. The inset is the enlargement of a part of the corresponding chromatogram. Experimental Conditions: substrate: 2-PAP; reactor: T316SS autoclave with stirring speed of 300 rpm; temperature: 260 °C; time: 4 h; Catalyst: None.

The hydrogen donating capability of the solvents severely affected both the conversion of 2-PAP and the product distribution (Fig. 2, S4, S5, and S6, Table 2). 2-PAP was almost entirely converted (> 99%) when AE or IPA were employed as solvents, whereas it was scarcely transformed (< 6%) when acetone or benzene were used as solvents (Fig. 2, Table 2). The distribution of the main products was different from each other in various solvents (Table 2, Table S4 and Fig. S5 in SI), which meant the transformation of 2-PAP proceeded along different pathways in solvents with different hydrogen donating capabilities.

Referring to published reports (Guthrie 1975; Netto-Ferreira *et al.* 1990; Andersen *et al.* 1996; Dorrestijn *et al.* 1999; Lanzalunga and Bietti 2000) and based on the main products' distribution listed in Fig. 2, Fig. S5, Table 2, and Table S4, a reaction network is proposed and illustrated in Scheme 2 to illuminate the plausible pathways involved in the decomposition of 2-PAP in different solvents in a T316SS autoclave.



Scheme 2. Illustration of active hydrogen transfer reactions promoted by stainless steel reactor

In this reaction network, the decomposition of 2-PAP proceeded along three routes, which were denoted as *Routes I, II, and III*, respective to various reaction solvents under different reaction conditions.

In solvents with high hydrogen donation ability, such as AE (Fig. 2A and S5A, and Entry 1 in Table 2), the decomposition of 2-PAP mostly proceeded along *Route I* (Dorrestijn *et al.* 1999). Essentially, the active hydrogen species generated from the solvents (illustrated in Scheme 1) participated in the proceedings and advanced the follow-up reactions (Guthrie 1975). The active hydrogen species (bonded to the surface of the steel wall, or as Metal-H) first attacked the oxygen atoms in α -carbonyl of the 2-PAP molecule and formed POPE radicals (Huang *et al.* 1995; Dorrestijn *et al.* 1999). The POPE radicals subsequently reacted along three routes, *Routes Ia, Ib, or Ic*, which led to further cleavage, rearrangement, or over-hydrogenation, respectively. According to the products' distribution of the decomposition of 2-PAP in AE offered in Tables 2 and S4, the POPE radicals split into phenoxy radicals and phenylethyl alcohol along *Route Ia* (Huang *et al.* 1995; Andersen *et al.* 1996; Lanzalunga and Bietti 2000). Then, the resultant 1-phenylethanol (an enol) further tautomerized to a more stable ketone form of acetophenone (AP in Scheme 2) (Huang *et al.* 1995), while the phenoxy radicals were terminated with the formation of phenol (P in Scheme 2) by abstracting hydrogen from acetophenone or the solvent (Netto-Ferreira *et al.* 1990). POPE radicals underwent isomerization along *Route Ib* and further cleaved to benzaldehyde along *Route Ib-1* (BAD in Scheme 2) (Dorrestijn *et al.* 1999). The intermediate of POPE radicals also isomerized, and then hydrogenated to generate 2-hydroxy-1,2-diphenylethan-1-one, which then further etherified into 2-ethoxy-1,2-diphenylethan-1-one (EDPE in Scheme 2) along *Route Ib-2*. POPE radicals also hydrogenated directly into POPE along *Route Ic* (Scheme 2). Ethyl benzoate (EBA in Scheme 2) was also detected in some cases, which was likely generated along *Route III* (Huang *et al.* 1995; Hanson *et al.* 2010). The detection of EBA was caused by a small amount of air remaining in the autoclave and the redox catalysis characteristics of the components in the stainless steel wall (Table S1) (Hanson *et al.* 2010).

As mentioned above, the reactions of 2-PAP in different kinds of autoclaves, such as a T316SS autoclave and a PPE-lined autoclave in static or dynamic mode and with or without a catalyst, showed a great diversity in the conversion and distribution of products, even in the same solvent. This meant that the stainless steel wall of the autoclave and the mass/heat transfer state both influenced the pathways of 2-PAP conversion. When the decomposition reaction was performed in a PPE-lined autoclave in dynamic mode without a dosage of SSP316 catalyst (Fig. 1D), the 2-PAP was partly hydrogenated to POPE along *Route Ic* with a small amount of cleavage. However, the addition of SSP316 in a PPE-lined autoclave as a catalyst improved the hydrogenation of 2-PAP to yield POPE, mostly *via Route Ic*, but there were low yields of the cleavage products, phenol and acetophenone (Fig. S2C). The stirring factor (mass transfer) also played an important role in the process of hydrogen transfer from the solvent to 2-PAP (comparing Fig. S2C and S2D). The promotion of mass transfer was clearly observed when comparing the results from the T316SS reactor at different stirring speeds (Fig. 1A-1C). The highest conversion of 2-PAP and selectivity of phenol and acetophenone was obtained in the T316SS autoclave with a stirring speed of 300 rpm (Fig. 1A), which indicated that *Route Ia* was the main reaction path under this condition.

Taking into consideration the results that acetal was produced independently of reactor type and stirring speed (Fig. S2E and S2F), it was easy to infer that the stainless steel wall of the autoclave did not contribute to the generation of hydrogen. Hence, a

possible explanation was that the stainless steel wall of the autoclave stabilized the intermediates of the reactions (*e.g.* POPE radicals, phenoxy radicals, and phenacyl radicals, *etc.* in Scheme 2) to suppress the side reactions (*Route Ib* in Scheme 2) or the excessive hydrogenation to stable POPE products (*Route Ic* in Scheme 2). Additionally, the stainless steel accelerated the hydrogen transfer to these intermediates. Vigorous stirring deeply affected the reaction pathway, and led to effective cleavage and delivery of hydrogen to intermediates that originated from ethanol. As a result, the high yields of the target products phenol and acetophenone (*Route Ia* in Scheme 2) were generated with decreased occurrences of rearrangement, isomerization, or excessive hydrogenation (*Routes Ib* and *Ic* in Scheme 2). Contrarily, while the reactions were performed in a PPE-lined autoclave without SSP316 as a catalyst, the intermediates (POPE radicals) formed by the reaction with hydrogen were so reactive that they either further hydrogenated to a stable product of POPE (*Route Ic* in Scheme 2) or rearranged and isomerized if they were not stabilized in time (Netto-Ferreira *et al.* 1990; Dorrestijn *et al.* 1999).

When the decomposition reaction was performed in solvents with poor hydrogen donation ability, such as acetone and benzene (Fig. 2C-D, and Entries 3 or 4 in Table 2), 2-PAP had to instead be pyrolyzed (homolyzed) and rearranged or recoupled along *Route II* (Table 2, Scheme 2 and Fig. S5) without the assistance of hydrogen species (Netto-Ferreira *et al.* 1990). Nevertheless, as the pyrolysis of β -O-4 bonds into radicals required much higher dissociation energy, this route was not easily accomplished and the cleavage efficiency was poor, which agreed highly with the low conversions listed in Table 2. Furthermore, the homolysis radicals were not stable and prone to recombination, disproportionation, or re-polymerization with the formation of some heavy fractions products if they were not terminated effectively by hydrogen or some other radical scavenger species (Netto-Ferreira *et al.* 1990).

Theoretically, the decomposition of 2-PAP should yield equal amounts of phenol and acetophenone (Scheme 1). However, when AE was employed as a solvent, it turned out that the selectivity of acetophenone was much lower than that of phenol, with a S_P/S_A ratio of 1.6, as shown in Table 2. The most probable explanation was that it was much easier for phenoxy radicals to abstract hydrogen from solvents or other sources with the formation of stable phenols under the current conditions (*Route Ia* in Scheme 2). Moreover, some other cleavage pathways of 2-PAP were also followed in which only phenol can be generated (*Route III* in Scheme 2, Table 2). Otherwise, acetophenone was not stable enough that it could be further transformed to 1-phenylethanol (PE in Scheme 2, Table 2 and Fig. S5) by hydrogenation along *Route Ia-1* or be abstracted hydrogen atoms to form acetophenone-radicals (Netto-Ferreira *et al.* 1990; Andersen *et al.* 1996; Park *et al.* 2011; Fan *et al.* 2015). The latter underwent dimerization or coupling reactions to form products with higher boiling points that could not be detected by GC-FID procedures (*Route Ia-2*) (DiNinno *et al.* 1977; Heathcock 1981; Netto-Ferreira *et al.* 1990). Furthermore, even the 2-acetylbenzoic acid was generated (ABA in Table S4 and Fig. S5) by a still unclear generation mechanism.

Moreover, compared with the decomposition in AE (Fig. 2A and Entry 1 in Table 2), the decomposition of 2-PAP proceeded better in IPA and had a higher conversion and selectivity of phenol (Fig. 2B and Entry 2 in Table 2). This was because the secondary alcohol had a higher hydrogen donation capability than the primary alcohol (Zassinovich *et al.* 1992), and much more active hydrogen was generated from IPA, which was beneficial for the activation and decomposition of 2-PAP. Unfortunately, the hydrogen yield derived from IPA caused an easier occurrence of side reactions, most likely along

Routes Ia-1 or Ib in Scheme 2 (Table 2 and Fig. S5) (Zassinovich *et al.* 1992; Sedai *et al.* 2013), and the generation of other products listed in Table S4 and Fig. S5, but not illustrated in Scheme 2. This led to a much lower selectivity of acetophenone than of phenol. It caused a higher ratio of S_P/S_A (2.4) and a small decrease in the mass yield ratio for other products.

Influence of Reaction Temperature

The influence of reaction temperature on the decomposition of 2-PAP was further investigated in a T316SS autoclave. The experiments were executed in AE for 4 h with a stirring speed of 300 rpm. With increased reaction temperature, the conversion of 2-PAP and the selectivity of phenol were both enhanced remarkably, while the selectivity of acetophenone, the S_P/S_A ratio, and the yield of other products exhibited a discrepancy (Table 3), which indicated that different pathways in the reaction network in Scheme 2 were followed.

Table 3. Data Analysis of Reaction Products with Increasing Temperature

Entry	Temperature (°C)	Conv. (%)	Products			
			S_P (%)	S_A (%)	S_P / S_A	Other mass yield (wt.%)
1	220	43.6	46.9	26.8	1.8	27.9
2	240	65.1	49.5	19.9	2.5	43.5
3	260	> 99	65.6	40.6	1.6	47.9
4	280	> 99	81.6	54.4	1.5	32.6

Experimental conditions: substrate: 2-PAP; reactor: T316SS autoclave with stirring speed of 300 rpm; solvent: AE; time: 4 h; Catalyst: None. Quantified by GC-FID using external standard method.

When the reactions were performed at 220 °C, 2-PAP conversion was only 43.6%, which indicated there was low hydrogen generation and depressed transfer activity of the T316SS at low temperatures. More importantly, the selectivities of both phenol and acetophenone were low, at only 46.9 and 26.8% (Table 3), respectively. These results most likely implied that at low temperatures the activity of T316SS for *Route Ia* path was limited and a lot of POPE radicals turned to benzaldehyde (BAD, *Route Ib-1*), 2-ethoxy-2-phenylacetophenone (EDPE, *Route Ib-2*), or POPE (*Route Ic*), which was verified by semi-quantitative data of the products' distribution (Table S5 and Fig. S7). Some 2-PAP molecules were oxidized to ethyl benzoate (EBA, *Route III*). Moreover, the selectivity of acetophenone was much lower than that of phenol with a S_P/S_A of 1.8, which could have been due to the fact there were more transformation pathways available for acetophenone, such as hydrogen abstraction and recoupling reactions, leading to the presence of some black floccules in the products (*Route Ia-2*, Fig. S8 in SI) (Fouassier and Lougnot 1987; Netto-Ferreira *et al.* 1990; Huang *et al.* 1995; Harwood *et al.* 2008). Also, there were more generation pathways available for phenol *via* oxidation in *Route III*.

When the reaction temperature was elevated to 240 °C, the conversion of 2-PAP was improved considerably, which was explained by the promotion of the hydrogen donation ability of AE and hydrogen transfer ability of T316SS along the *Route I* path. However, the selectivity of phenol only slightly increased (49.5%), whilst the selectivity of acetophenone decreased to 19.9%, which led to a tremendous increase of the S_P/S_A ratio (2.5) and a slight increase in the mass yield of other products (Table 3). Referring to the semi-quantitative data in Table S5, it was found that the increase of the 2-PAP conversion

did not result from reactions along *Route Ia* and *Ib*, but was mainly caused by the increasing amount of hydrogenation to POPE along *Route Ic* in Scheme 2, which resulted in only a slight increase in the yield of phenol. The phenomenon that acetophenone selectivity was even less than at 220 °C was attributed to the increased rate of recoupling reaction of acetophenone at this temperature (*Route Ia-2* in Scheme 2), as verified by the presence of more black floccules in the products (Fig. S7 in SI).

As the reaction temperature was further elevated to 260 °C, the conversion of 2-PAP and the selectivity of phenol and acetophenone were all enhanced, and the S_P/S_A ratio (1.6) and the yields of other products were both decreased. These phenomena demonstrated the noticeably enhanced activities of hydrogen generation and hydrogen transfer of the T316SS wall, which resulted in the conversion of 2-PAP preferentially along *Route Ia*, led to the high yield and selectivity of the cleavage products, phenol and acetophenone. The decrease in the S_P/S_A ratio was ascribed to the relatively low tendencies of hydrogen abstraction and recoupling reactions along *Route Ia-2*, as verified by the almost complete disappearance of black floccules in the products (Fig. S7). This was despite the fact that hydrogenation reactions along *Route Ia-1* were enhanced, as evidenced by the generation of 1-phenylethanol as shown in Table S5. Moreover, the elevated temperature also promoted the side reactions along *Route Ib* and *III*. A tremendous reduction in the tendency of *Route Ic* was observed by the competition of various pathways in the reaction network, which led to a smaller increase in the yield of other products.

As the reaction temperature increased to 280 °C, the selectivities of phenol and acetophenone simultaneously increased, but the S_P/S_A ratio remained mostly unchanged (Table 3). These results were explained by the further enhancement of reactions along *Route Ia* due to increased hydrogen generation from AE and the hydrogen transfer ability of the wall of the T316SS autoclave reactor (Samec *et al.* 2006; Toubiana and Sasson 2012). Furthermore, the reactions along *Route Ia-2* mostly vanished with a clearer solution after the reaction (Fig. S7), although some excessive hydrogenation products appeared, such as styrene, ethyl α -methylbenzyl ether, and ethyl benzoate, appeared (*Route Ia-1*, Table S5), and the reactions along *Route Ib-1* and *III* proceeded to generate 4-(hydroxyethyl)benzaldehyde and ethyl benzenecarboxylate (Table S5). As a result, the mass yield of others products decreased to 32.6% (Table 3), which implied that elevating the temperature benefited the enhancement of yield and selectivity of target cleavage products.

Further Investigation with Additional Catalyst

The stainless steel behaved as an efficient catalyst at intermediate to high temperatures in the aforementioned reactions. Some literature reported that the presence of an acid or base further promoted reactions, such as dry-reforming of ethanol (Samec *et al.* 2006; Toubiana and Sasson 2012). Increased surface acid sites also promoted the decomposition of β -O-4 linked lignin model compound (Kim *et al.* 2014). Therefore, further investigation was carried out using $Cs_{2.5}H_{0.5}PMo_{12}O_{40}$ as a co-catalyst to improve the decomposition of 2-PAP. The reactions were also conducted in AE at the prescribed temperature for 4 h in a T316SS autoclave with a stirring speed of 300 rpm.

Compared with the results without any catalyst (Table 3), the addition of $Cs_{2.5}H_{0.5}PMo_{12}O_{40}$ greatly enhanced the decomposition of 2-PAP at the lowest reaction temperature, 240 °C, improved selectivities of cleavage products, and decreased the yield of by-products (Table 4). At high reaction temperatures, 2-PAP was almost completely converted to the desired products with a S_P/S_A ratio of 1.1. These results showed that the

addition of $\text{Cs}_{2.5}\text{H}_{0.5}\text{PMo}_{12}\text{O}_{40}$ further promoted the cleavage of the β -O-4 bond and improved the hydrogen transfer efficiency from AE to intermediates to generate phenol and acetophenone (Park *et al.* 2011) and thus inhibited possible side reactions. At 280 °C, the selectivity of phenol and acetophenone reached 98.6% and 91.1%, respectively, with a conversion of 2-PAP greater than 99%, and the mass yield of other products was 4.6 wt.%.

Table 4. Further Investigation using $\text{Cs}_{2.5}\text{H}_{0.5}\text{PMo}_{12}\text{O}_{40}$ as Co-Catalyst

Catalyst	Temperature (°C)	Conv. (%)	Products			
			S _P (%)	S _A (%)	S _P /S _A	Other mass yield (wt.%)
$\text{Cs}_{2.5}\text{H}_{0.5}\text{PMo}_{12}\text{O}_{40}$	240	86.4	66.0	39.1	1.7	42.0
$\text{Cs}_{2.5}\text{H}_{0.5}\text{PMo}_{12}\text{O}_{40}$	260	> 99	79.9	58.6	1.4	31.4
$\text{Cs}_{2.5}\text{H}_{0.5}\text{PMo}_{12}\text{O}_{40}$	280	> 99	98.6	91.1	1.1	4.6

Experimental conditions: substrate: 2-PAP; reactor: T316SS autoclave with stirring speed of 300 rpm; solvent: AE; temperature: 260 °C; time: 4 h; Quantified by GC-FID using external standard method.

The discovery that stainless steel promoted hydrogen transfer reactions in this study revealed the merits of a high conversion efficiency and selectivity, as well as easy handling without the need for noble metals and complicated catalysts. The proposed method of the decomposition of 2-PAP in a stainless steel reactor with the aid of polyoxometalates may be employed to develop a promising process for the decomposition of lignin to valuable multi-functional unsaturated benzenes. Some inspiring results were obtained in this study. A systematic investigation is still in progress.

CONCLUSIONS

1. The cleavage of a lignin model compound of 2-PAP in hydrogen donation solvents with a high conversion of 2-PAP (> 99%) was achieved with impressive selectivity of desired products (> 80% for phenol) without the addition of any catalyst.
2. The proposed reaction network was shown to have an active hydrogen transfer process, which was effectively promoted by the stainless steel.
3. The intensive investigation demonstrated that the active hydrogen liberated from AE transferred to 2-PAP, which promoted the cleavage reaction of 2-PAP and stabilized the intermediates. This decreased the occurrence of rearrangement, recoupling, and condensation.
4. Further investigation demonstrated that the addition of $\text{Cs}_{2.5}\text{H}_{0.5}\text{PMo}_{12}\text{O}_{40}$ as a co-catalyst further enhanced the conversion (> 99%) of 2-PAP and selectivity (91%) of the target products.

ACKNOWLEDGMENTS

This work is supported by the International Science and Technology Cooperation Projects of Guangxi, China (15104001-5), National Key Basic Research Program of China

(2013CB934101), NSFC (21433002, 21573046, 21473037, and U1463206), Sinopec (X514005), and National Plan for Science and Technology of Saudi Arabia (14-PET827-02).

REFERENCES CITED

- Andersen, M. L., Mathivanan, N., and Wayner, D. D. M. (1996). "Electrochemistry of electron-transfer probes. The role of the leaving group in the cleavage of radical anions of α -aryloxyacetophenones," *J. Am. Chem. Soc.* 118(20), 4871-4879. DOI: 10.1021/ja954093+
- Argyropoulos, D. S. (2007). *Materials, Chemicals, and Energy from Forest Biomass*, American Chemical Society, Washington, DC.
- Bull, T. E. (1999). "Biomass in the energy picture," *Science* 285(5431), 1209. DOI: 10.1126/science.285.5431.1209b
- De Oliveira-Vigier, K., Abatzoglou, N., and Gitzhofer, F. (2005). "Dry-reforming of ethanol in the presence of a 316 stainless steel catalyst," *Can. J. Chem. Eng.* 83(6), 978-984. DOI: 10.1002/cjce.5450830607
- Deuss, P. J., and Barta, K. (2016). "From models to lignin: Transition metal catalysis for selective bond cleavage reactions," *Coordin. Chem. Rev.* 306(Part 2), 510-532. DOI: 10.1016/j.ccr.2015.02.004
- DiNinno, F., Beattie, T. R., and Christensen, B. G. (1977). "Aldol condensations of regiospecific penicillanate and cephalosporanate enolates – Hydroxyethylation at C-6 and C-7," *J. Org. Chem.* 42(18), 2960-2965. DOI: 10.1021/jo00438a003
- Dorrestijn, E., Hemmink, S., Hulstman, G., Monnier, L., van Scheppingen, W., and Mulder, P. (1999). "The reduction of alpha-X-acetophenones (X= PhO, Br, Cl) in hydrogen-donating solvents at elevated temperatures," *Eur. J. Org. Chem.* 1999(3), 607-616. DOI: 10.1002/(SICI)1099-0690(199903)1999:3<607::AID-EJOC607>3.0.CO;2-V
- Dutta, S., Wu, K. C. W., and Saha, B. (2014). "Emerging strategies for breaking the 3D amorphous network of lignin," *Catal. Sci. Technol.* 4(11), 3785-3799. DOI: 10.1039/C4CY00701H
- Fan, H., Yang, Y., Song, J., Meng, Q., Jiang, T., Yang, G., and Han, B. (2015). "Free-radical conversion of a lignin model compound catalyzed by Pd/C," *Green Chem.* 17(8), 4452-4458. DOI: 10.1039/C5G01272D
- Fouassier, J. P., and Lougnot, D. J. (1987). "Excited-state reactivity in a series of polymerization photoinitiators based on the acetophenone nucleus," *J. Chem. Soc. Farad. T.* 183(9), 2935-2952. DOI: 10.1039/F19878302935
- Guthrie, J. P. (1975). "Carbonyl addition reactions: Factors affecting the hydrate-hemiacetal and hemiacetal-acetal equilibrium constants," *Can. J. Chem.* 53(6), 898-906. DOI: 10.1139/v75-125
- Hanson, S. K., Baker, R. T., Gordon, J. C., Scott, B. L., and Thorn, D. L. (2010). "Aerobic oxidation of lignin models using a base metal vanadium catalyst," *Inorg. Chem.* 49(12), 5611-5618. DOI: 10.1021/ic100528n
- Harwood, H. J., McNamara, K., Johnson, J. J., and Wyzgoski, F. J. (2008). "Initiator selectivity during free radical copolymerizations of styrene and methyl methacrylate initiated by anaerobic copper(II) oxidation of carbon-13 labeled acetophenone," *J. Polym. Sci. Pol. Chem.* 46(7), 2347-2356. DOI: 10.1002/pola.22567

- Heathcock, C. H. (1981). "Acyclic stereocontrol through the aldol condensation," *Science* 214(4519), 395-400. DOI: 10.1126/science.214.4519.395
- Heitner, C., Dimmel, D. R., and Schmidt, J. A. (2010). *Lignin & Lignans: Advances in Chemistry*, CRC Press, Boca Raton, FL.
- Huang, Y., Pagé, D., Wayner, D. D. M., and Mulder, P. (1995). "Radical-induced degradation of a lignin model compound. Decomposition of 1-phenyl-2-phenoxyethanol," *Can. J. Chem.* 73(11), 2079-2085. DOI: 10.1139/v95-256
- Huang, X., Korányi, T. I., Boot, M. D., and Hensen, E. J. M. (2015). "Ethanol as capping agent and formaldehyde scavenger for efficient depolymerization of lignin to aromatics," *Green Chem.* 17(11), 4941-4950. DOI: 10.1039/C5GC01120E
- Kang, S., Li, X., Fan, J., and Chang, J. (2013). "Hydrothermal conversion of lignin: A review," *Renew. Sust. Energ. Rev.* 27, 546-558. DOI: 10.1016/j.resr.2013.07.013
- Kim, J. K., Park, H. W., Hong, U. G., Choi, J. H., and Song, I. K. (2014). "CSxH3.0-xPW12O40 (X=2.0-3.0) heteropolyacid nano-catalysts for catalytic decomposition of 2,3-dihydrobenzofuran to aromatics," *Journal of Nanoscience and Nanotechnology* 14(11), 8884-8890. DOI: 10.1166/jnn.2014.9947
- Lanzalunga, O., and Bietti, M. (2000). "Photo-and radiation chemical induced degradation of lignin model compounds," *J. Photoch. Photobio. B* 56(2-3), 85-108. DOI: 10.1016/S1011-1344(00)00054-3
- Luo, Z., Wang, Y., He, M., and Zhao, C. (2016). "Precise oxygen scission of lignin derived aryl ethers to quantitatively produce aromatic hydrocarbons in water," *Green Chem.* 18(2), 433-441. DOI: 10.1039/C5GC01790D
- Netto-Ferreira, J. C., Avellar, I. G. J., and Scaiano, J. C. (1990). "Effect of ring substitution on the photochemistry of α -(aryloxy) acetophenones," *J. Org. Chem.* 55(1), 89-92. DOI: 10.1021/jo00288a019
- Park, H. W., Park, S., Park, D. R., Choi, J. H., and Song, I. K. (2011). "Catalytic decomposition of benzyl phenyl ether to aromatics over cesium-exchanged heteropolyacid catalyst," *Korean J. Chem. Eng.* 28(5), 1177-1180. DOI: 10.1007/s11814-010-0491-1
- Samec, J. S., Bäckvall, J.-E., Andersson, P. G., and Brandt, P. (2006). "Mechanistic aspects of transition metal-catalyzed hydrogen transfer reactions," *Chem. Soc. Rev.* 35(3), 237-248. DOI: 10.1039/B515269K
- Sedai, B., Diaz-Urrutia, C., Baker, R. T., Wu, R., Silks, L. A., and Hanson, S. K. (2013). "Aerobic oxidation of β -1 lignin model compounds with copper and oxovanadium catalysts," *ACS Catalysis* 3(12), 3111-3122. DOI: 10.1021/cs400636k
- Song, Q., Wang, F., Cai, J., Wang, Y., Zhang, J., Yu, W., and Xu, J. (2013). "Lignin depolymerization (LDP) in alcohol over nickel-based catalysts via a fragmentation-hydrogenolysis process," *Energ. Environ. Sci.* 6(3), 994-1007. DOI: 10.1039/C2EE23741E
- Strassberger, Z., Alberts, A. H., Louwense, M. J., Tanase, S., and Rothenberg, G. (2013). "Catalytic cleavage of lignin β -O-4 link mimics using copper on alumina and magnesia-alumina," *Green Chem.* 15(3), 768-774. DOI: 10.1039/C3GC37056A
- Szpyrkowicz, L., Ricci, F., Montemor, M. F., and Souto, R. M. (2005). "Characterization of the catalytic films formed on stainless steel anodes employed for the electrochemical treatment of cuprocyanide wastewaters," *J. Hazard. Mater.* 119(1-3), 145-152. DOI: 10.1016/j.jhazmat.2004.11.015
- Toubiana, J., and Sasson, Y. (2012). "The true catalyst in hydrogen transfer reactions with alcohol donors in the presence of RuCl₂(PPh₃)₃ is ruthenium(0) nanoparticles," *Catal.*

- Sci. Technol.* 2(8), 1644-1653. DOI: 10.1039/C2CY00514J
- van Haveren, J., Scott, E. L., and Sanders, J. (2008). "Bulk chemicals from biomass," *Biofuel. Bioprod. Bioref.* 2(1), 41-57. DOI: 10.1002/bbb.43
- Vollhardt, K. P. C., and Schore, N. E. (2011). *Organic Chemistry: Structure and Function*, W. H. Freeman, New York, NY.
- Werpy, T., Petersen, G., Aden, A., Bozell, J., Holladay, J., White, J., Manheim, A., Eliot, D., Lasure, L., and Jones, S. (2004). *Top Value Added Chemicals from Biomass. Volume 1-Results of Screening for Potential Candidates from Sugars and Synthesis Gas* (DOE/GO-102004-1992), U.S. Department of Energy, Washington, DC.
- Xu, W., Miller, S. J., Agrawal, P. K., and Jones, C. W. (2012). "Depolymerization and hydrodeoxygenation of switchgrass lignin with formic acid," *ChemSusChem* 5(4), 667-675. DOI: 10.1002/cssc.201100695
- Yan, N., Yuan, Y., Dykeman, R., Kou, Y., and Dyson, P. J. (2010). "Hydrodeoxygenation of lignin-derived phenols into alkanes by using nanoparticle catalysts combined with brønsted acidic ionic liquids," *Angew. Chem. Int. Ed.* 49(32), 5549-5553. DOI: 10.1002/anie.201001531
- Zakzeski, J., Jongerijs, A. L., Bruijninx, P. C., and Weckhuysen, B. M. (2012). "Catalytic lignin valorization process for the production of aromatic chemicals and hydrogen," *ChemSusChem* 5(8), 1602-1609. DOI: 10.1002/cssc.201100699
- Zassinovich, G., Mestroni, G., and Gladiali, S. (1992). "Asymmetric hydrogen transfer reactions promoted by homogeneous transition metal catalysts," *Chem. Rev.* 92(5), 1051-1069. DOI: 10.1021/cr00013a015
- Zeng, J., Yoo, C. G., Wang, F., Pan, X., Vermerris, W., and Tong, Z. (2015). "Biomimetic fenton-catalyzed lignin depolymerization to high-value aromatics and dicarboxylic acids," *ChemSusChem* 8(5), 861-871. DOI: 10.1002/cssc.201403128
- Zhang, J., Liu, Y., Chiba, S., and Loh, T.-P. (2013). "Chemical conversion of β -O-4 lignin linkage models through Cu-catalyzed aerobic amide bond formation," *Chem. Commun.* 49(97), 11439-11441. DOI: 10.1039/C3CC46912C

Article submitted: August 13, 2016; Peer review completed: October 6, 2016; Revised version received and accepted: October 20, 2016; Published: October 25, 2016.
DOI: 10.15376/biores.11.4.10349-10377

APPENDIX: SUPPORTING INFORMATION

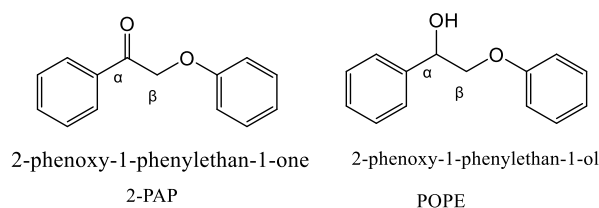


Fig. S1. Molecular structures of model compounds 2-PAP and POPE

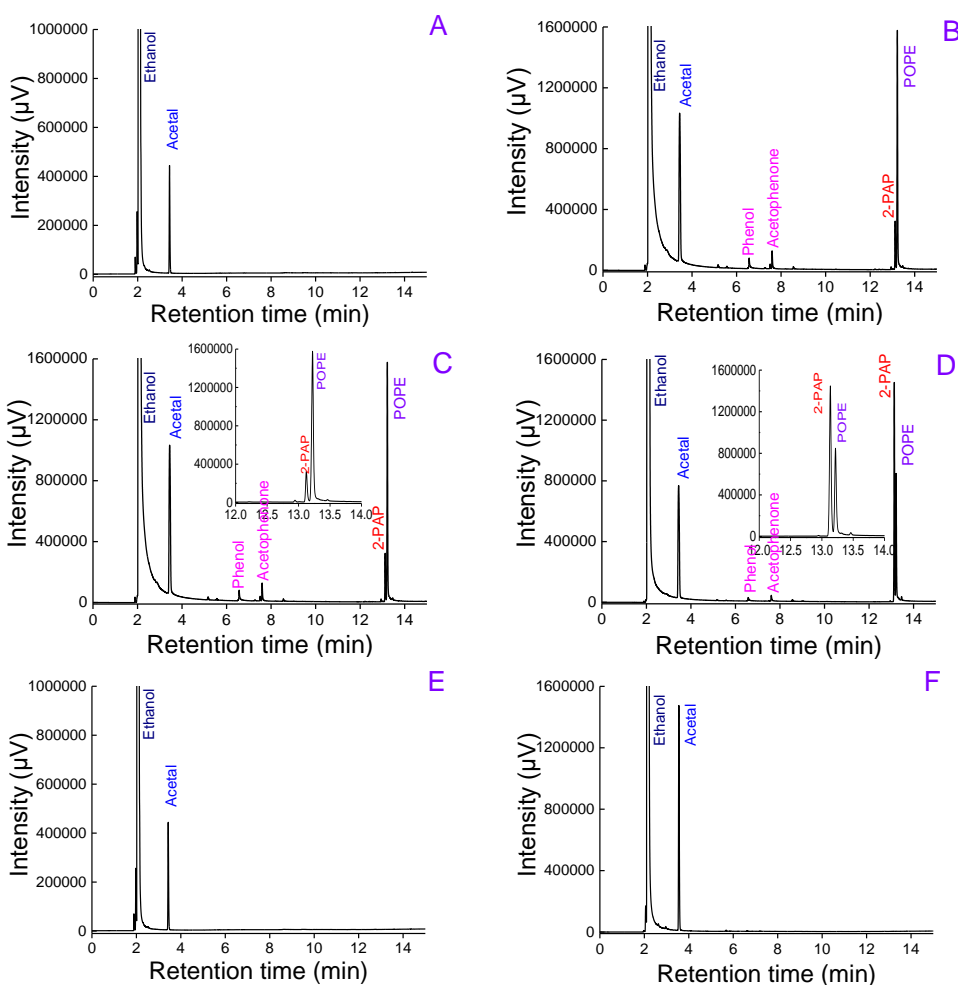


Fig. S2. Chromatograms of blank AE, raw materials or post-reaction products detected by GC-FID method and qualified by GC-MS method: (A) bank anhydrous ethanol; (B) raw material (and standard) of 2-PAP dissolved in AE; (C) 2-PAP-SSP316-AE-260 °C-4 h- dynamic mode-in PPE-lined; (D) 2-PAP-SSP316-AE-260 °C-4 h- static mode-in PPE-lined; (E) pure AE proceeded in T316SS autoclave at 260 °C for 4 h without additional catalyst with stirring speed of 300 rpm; (F) pure AE proceeded in PPE-lined autoclave at 260 °C for 4 h at static mode;. The inset in Figures C, D is the enlargement of a part of the correspondence chromatogram; *AE: anhydrous ethanol; PPE: poly(phenylene).

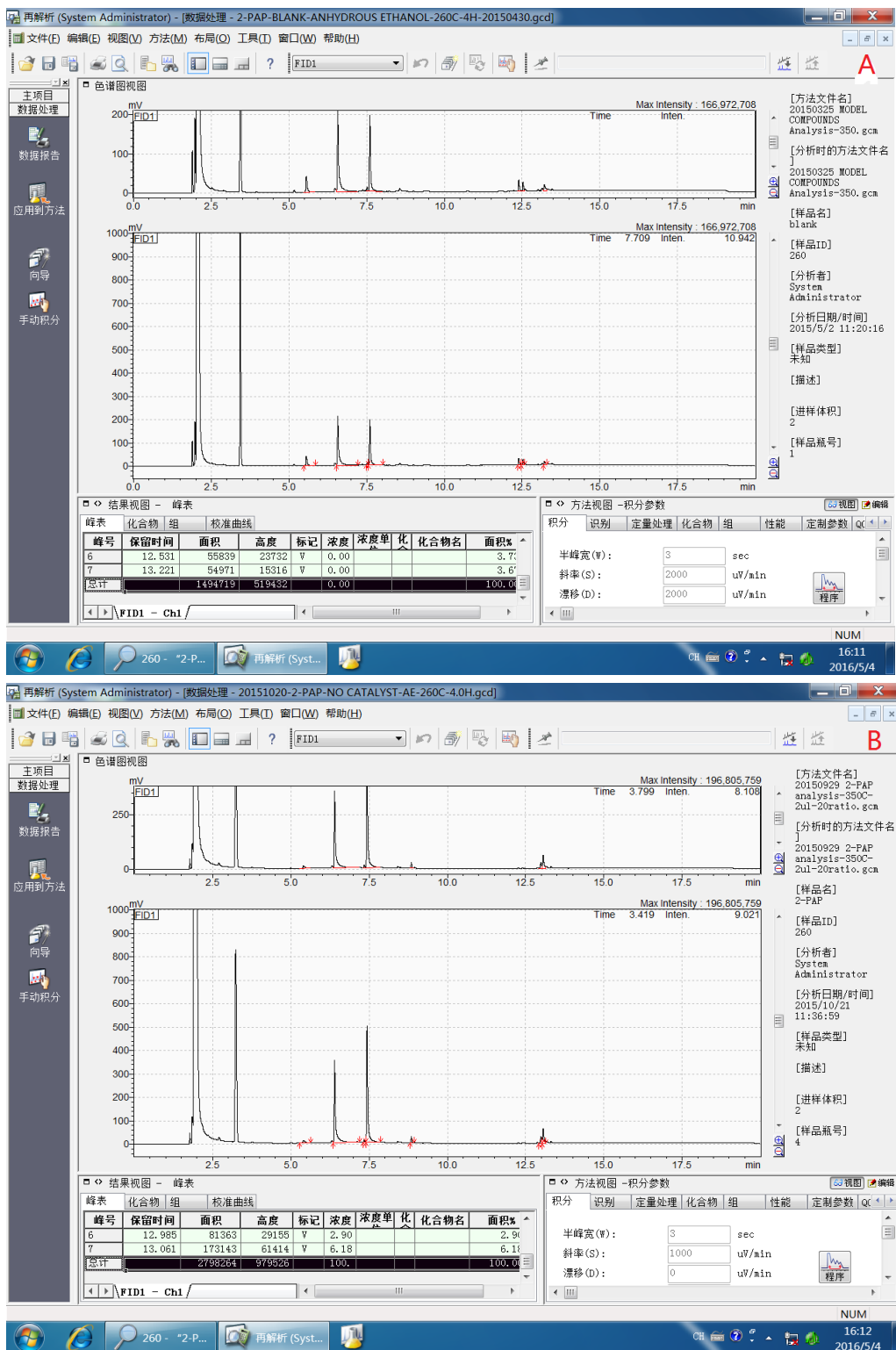


Fig. S3. The captures of original GC-FID analysis of repetitive test of 2-PAP decomposition in AE at 260 °C for 4 h with stirring speed of 300 rpm without added any catalyst: (A) reaction conducted on 30th, Apr., 2015; (B) reaction conducted on 20 October 2015

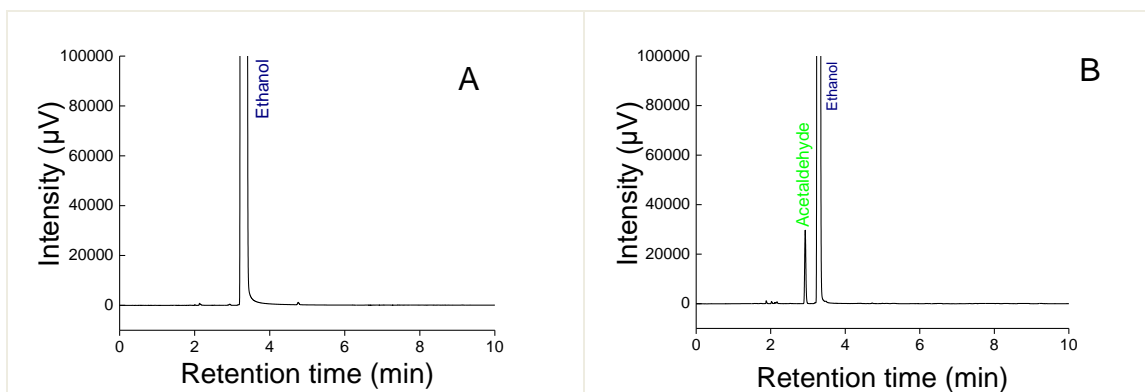
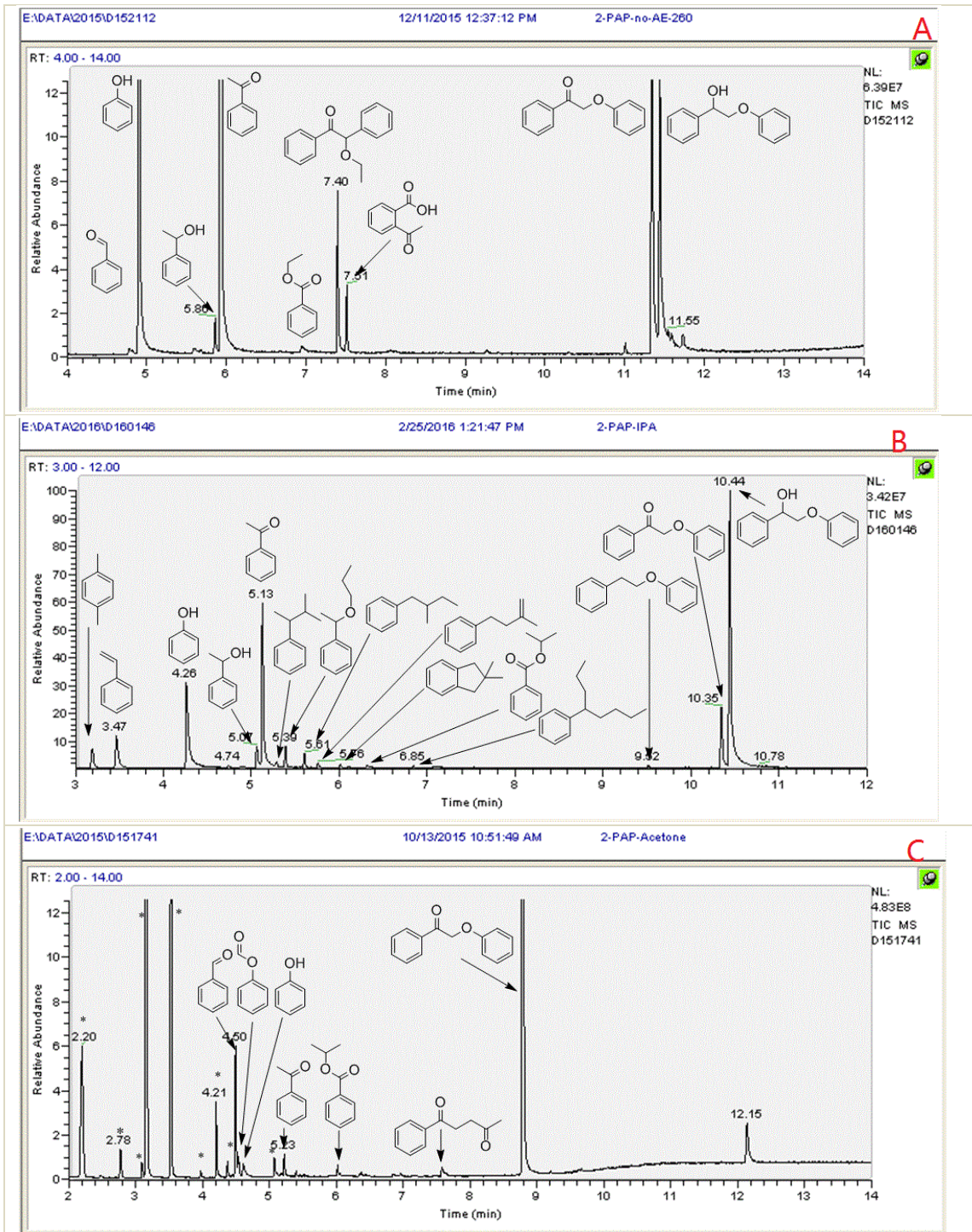


Fig. S4. GC-FID chromatograms of blank anhydrous ethanol (AE) (A) before and (B) after reaction in T316SS autoclave with stirring speed of 300 rpm at 260 °C for 4 h

Because the acetic aldehyde cannot be separated from ethanol in the column of HP-5, as those shown in Figs. 1A or 1I, the chromatograms in Fig. S4 were analyzed on another GC-FID (Shimadzu, GC-2010) equipped with a DKM-FFAP column (30 m × 0.25 mm × 0.5 μm). It was shown that the concentration of acetaldehyde in pure AE before reaction was < 0.001% by a semi-quantitative normalization method, while that after thermal treatment in a T316SS autoclave at 260 °C for 4 h remarkably increased to 0.336%.



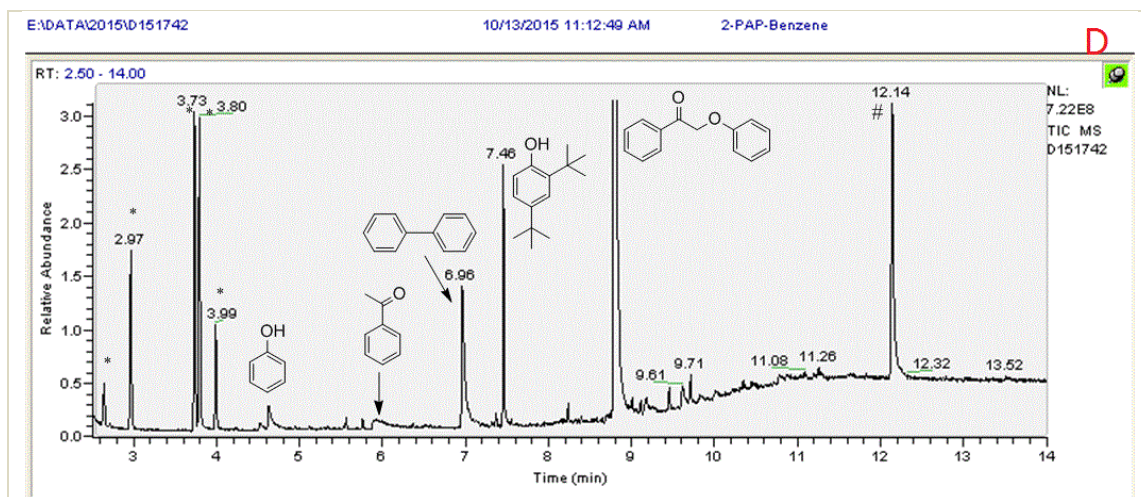


Fig. S5. Total ion current profiles from GC-MS of reactions products of 2-PAP in the solvents of (A) AE, (B) IPA, (C) acetone and (D) benzene in T316SS autoclave with stirring speed of 300 rpm and no additional catalyst at 260 °C for 4 h

* Peak for the products from solvent itself

Peak of high-vacuum grease

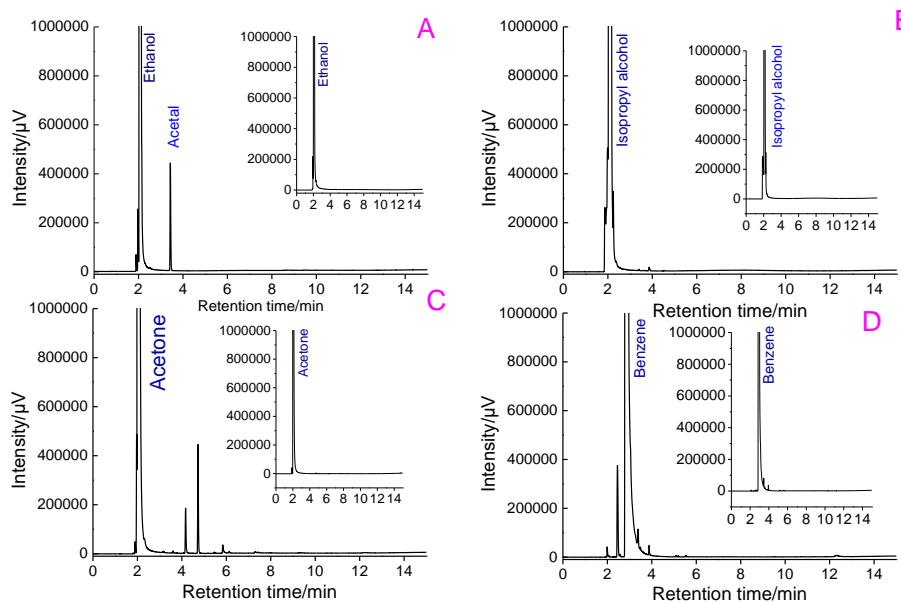


Fig. S6. GC-FID Chromatograms of blank solvents after control reactions: (A) AE; (B) IPA; (C) Acetone; (D) Benzene. The **insets** show the profiles of the correspondent blank solvent without processing.

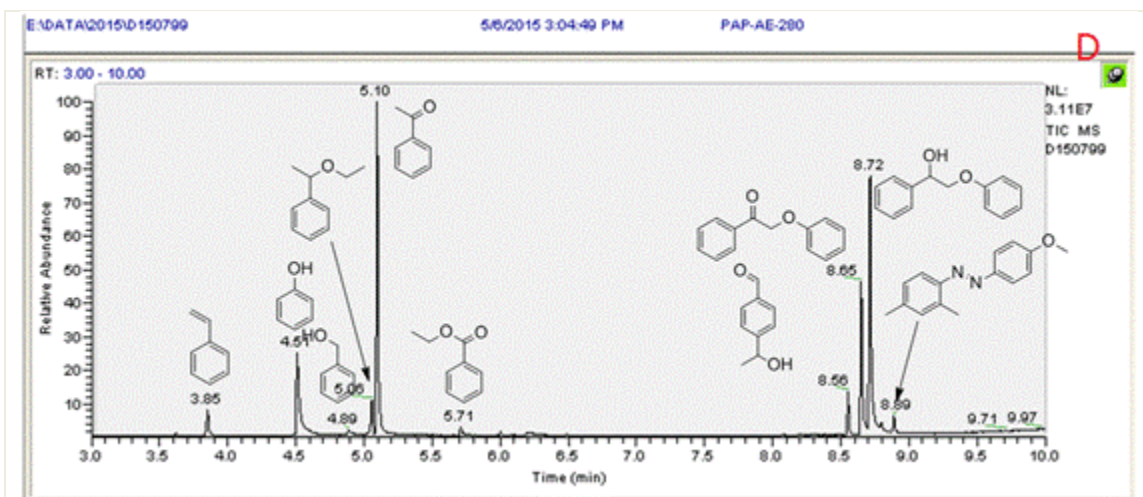


Fig. S7. Total ion current profiles from GC-MS of reactions products of 2-PAP in AE in T316SS autoclave with stirring speed of 300 rpm and no additional catalyst at (A) 220, (B) 240, (C) 260 and (D) 280 °C * for 4 h.

*This TIC profiles were collected under different programmed temperature procedure conditions of GC-MS before the others.

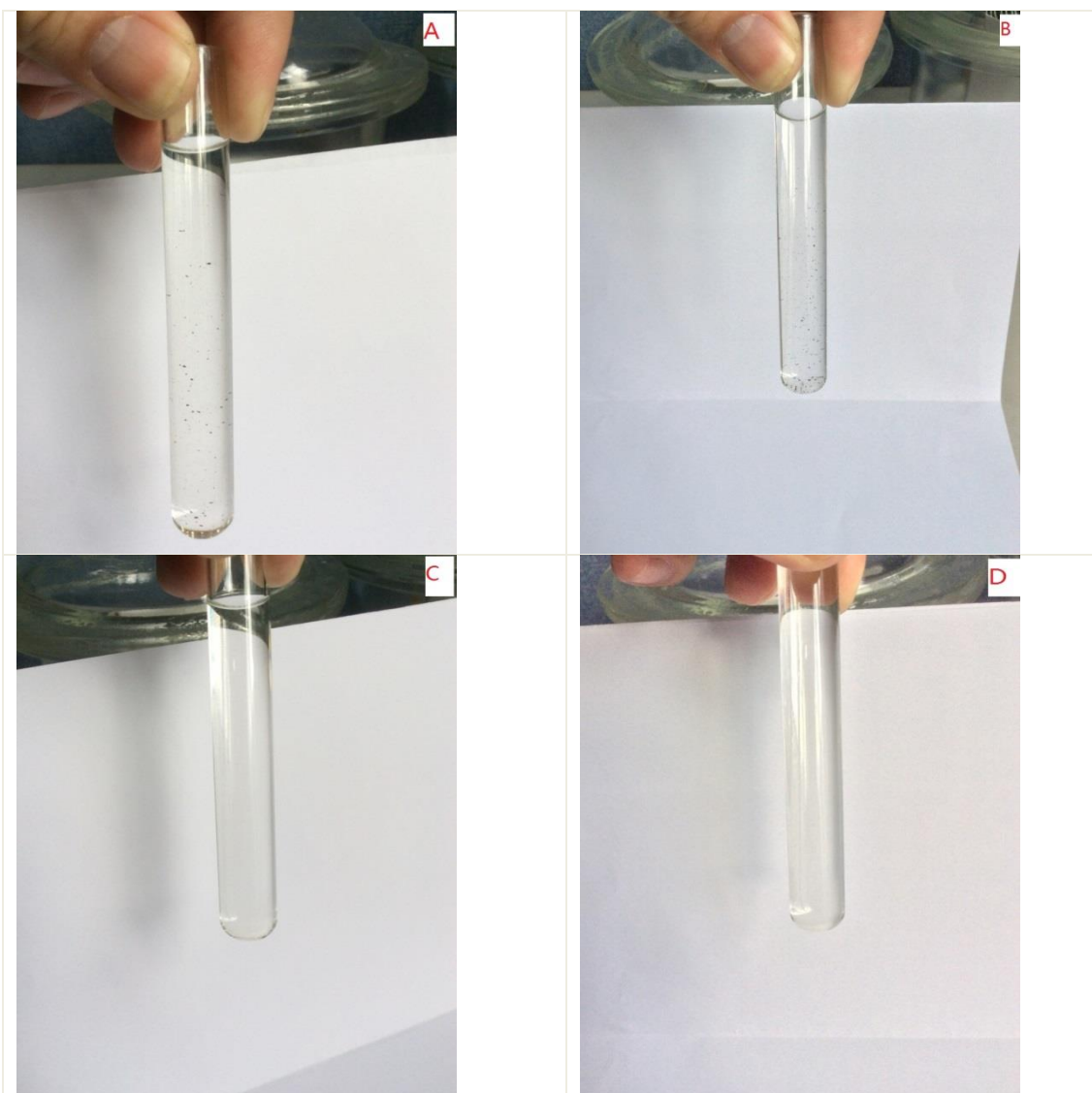


Fig. S8. Photos of suspending liquids after reactions of 2-PAP in AE in T316SS autoclave with stirring speed of 300 rpm and no additional catalyst at (A) 220, (B) 240, (C) 260 and (D) 280 °C for 4 h

Table S1. Nominal Chemical Composition of T316SS Pressure Vessel Materials (Parr Instrument)

Material	Typical trade name	Composition (wt.%)						
		Fe	Ni	Cr	Mo	Mn	Si	Others
T316 stainless steel	T316SS	65	12	17	2.5	2.0	1.0	<0.5
316 powder	SSP316	64~68	12~14	16~18	2~3	2~3	≤ 1.0	<0.5

Table S2. Detailed Retention Time of the Main Compounds Involved in the Reactions

Compound	Retention time (min)
AE	1.914
IPA	2.183
Acetone	1.874
Benzene	2.872
Acetal	3.437
Phenol	6.433
Acetophenone	7.475
2-PAP	13.134
POPE	13.215

Table S3. Concentrations of Metals Dissolved in AE Before and After Reaction*

Element	Concentration before reaction (mg/L)	Concentration post-reaction (mg/L)	Detection limit (mg/L)
Fe	0.02	0.048	0.002
Si	0.08	0.07	0.008
Ni	n.d.#	n.d.	0.008
Mo	n.d.	n.d.	0.004
Mn	n.d.	n.d.	0.0005
Cr	n.d.	n.d.	0.003

* All metal components concentrations were simultaneously determined by ICP-AES.

n.d. not detected.

Table S4. Main Product Distribution of Decomposition of 2-PAP in Various Solvents

AE		Acetone		Benzene		IPA
Product	Labeling	Product	Labeling	Product	Labeling	Product
benzaldehyde	BAD	benzaldehyde	BAD	benzaldehyde	BAD	styrene
phenol	P	phenol	P	phenol	P	phenol
acetophenone	AP	acetophenone	AP	acetophenone	AP	1-phenylethanol
2-ethoxy-1,2-diphenyl-ethanone	EDPE	2-PAP	2-PAP	benzoic acid	BA	acetophenone
2-acetylbenzoic acid	ABA			biphenyl	BP	2-methyl-3-phenyl-butane
Ethyl benzenecarboxylate	EBA			2-PAP	2-PAP	(1-propoxyethyl)benzene
1-phenylethanol	PE					2-methyl-1-phenyl-butane
2-PAP	2-PAP					2-methyl-4-phenyl-butene
POPE	POPE					2,3-dihydro-2,2-dimethyl-1H-indene
						Isopropyl ester benzoic acid
						4-phenyl-octane
						(2-phenoxyethyl)benzene
						2-PAP
						POPE

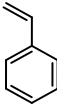
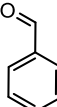
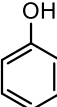
Experimental conditions: substrate: 2-PAP; reactor: T316SS autoclave with stirring speed of 300 rpm; solvent: AE; temperature: 260 °C; time: 4 h; Catalyst: None.

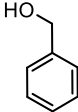
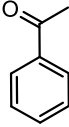
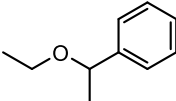
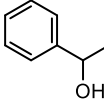
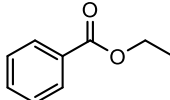
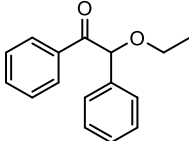
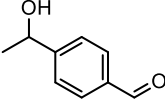
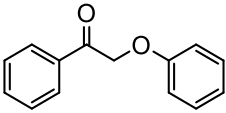
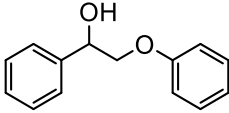
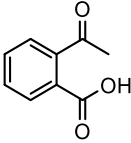
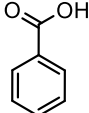
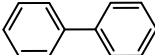
Table S5. Semi-Quantified By-Products from Decomposition of 2-PAP in AE at Various Temperatures

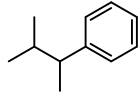
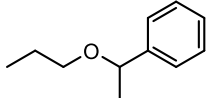
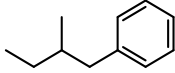
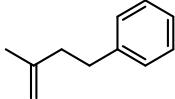
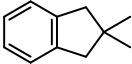
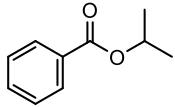
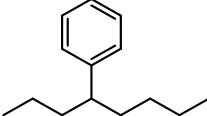
By-product	Peak area of total ion current of GC-MS							
	220 °C		240 °C		260 °C		280 °C	
	Area	Plausible route	Area	Plausible route	Area	Plausible route	Area	Plausible route
Styrene	n.d.	-	n.d.	-	n.d.	-	1175578	la-1
Benzaldehyde	499012	lb-1	504351	lb-1	326235	lb-1	n.d.	-
benzenemethanol	n.d.	-	n.d.	-	457550	III	179646	III
Ethyl α -methylbenzyl ether	n.d.	-	n.d.	-	n.d.	-	1578831	la-1
1-phenylethanol	n.d.	-	n.d.	-	1031095	la-1	n.d.	-
Ethyl benzenecarboxylate	703317	III	325387	III	609016	III	1610920	III
2-ethoxy-2-phenylacetophenone	2029877	lb-2	1268545	lb-2	5352527	lb-2	n.d.	-
4-(1-hydroxyethyl) benzaldehyde	n.d.	-	n.d.	-	n.d.	-	1687361	lb-1
POPE	8499890	lc	21232945	lc	13039369	lc	14821145	lc
2-acetylbenzoic acid	196236		201811		1837162		n.d.	-

Experimental conditions: substrate: 2-PAP; reactor: T316SS autoclave with stirring speed of 300 rpm; solvent: AE; time: 4 h; Catalyst: None. Qualified by GC-MS (acetal in anhydrous ethanol is not included).

Table S6. Names and Corresponding Molecular Structures of Main Products

Name	Structure
styrene	
benzaldehyde	
phenol	

benzenemethanol	
acetophenone	
ethyl α -methylbenzyl ether	
1-phenylethanol	
ethyl benzenecarboxylate	
2-ethoxy-2-phenyl- acetophenone	
4-(1-hydroxyethyl)benzaldehyde	
2-PAP	
POPE	
2-acetylbenzoic acid	
benzoic acid	
biphenyl	

2-methyl-3-phenylbutane	
(1-propoxyethyl)benzene	
(2-methylbutyl)benzene	
2-methyl-4-phenyl-but-1-ene	
2,3-dihydro-2,2-dimethyl-1H-indene	
Isopropyl benzoate	
4-phenyloctane	
(2-phenoxyethyl)benzene	